

Single quantum-dot Purcell factor and β factor in a photonic crystal waveguide

V. S. C. Manga Rao and S. Hughes*

Department of Physics, Queen's University, Kingston, Ontario, Canada K7L 3N6

(Received 22 December 2006; published 24 May 2007)

A theoretical formalism to calculate the spontaneous emission rate enhancement (Purcell factor) and propagation mode β factor from single quantum dots in a planar-photonic-crystal waveguide is presented. Large Purcell factors for slow light modes, and enormous β factors (>0.85) over a broadband (10 THz) spectral range are subsequently predicted. The local density of photon states is found to diverge at the photonic band edge, but we discuss why this divergence will always be broadened in real samples, most notably due to structural disorder. Applications towards “on-chip” single photon sources are highlighted.

DOI: [10.1103/PhysRevB.75.205437](https://doi.org/10.1103/PhysRevB.75.205437)

PACS number(s): 68.65.Hb, 42.55.Tv, 78.67.Hc

I. INTRODUCTION

Future quantum information processing architectures, quantum networks, and teleportation schemes,^{1–4} as well as quantum key distributions for secure communication,⁵ will rely on producing efficient and deterministic single-photon sources.^{2,6} Ideally, a single photon should be found in a single mode with well-defined spatial and temporal characteristics. The desired single-photon on demand should exhibit strict quantum-mechanical behavior such as antibunching, indistinguishability, and sub-Poissonian statistics.⁶ Recently, numerous schemes have been proposed and demonstrated for producing single-photon sources including single atoms in a high-finesse cavity,⁷ single molecules,^{8,9} atomic ensembles,¹⁰ nitrogen vacancies in a diamond nanocrystal,⁵ and trapped ions.¹¹ In all of these reported schemes, the photon extraction (or collection efficiency), as well as issues relating to scalability and integrability, remain major problems for any practical device or future implementation. It is thus a remaining concern to find new material structures that not only produce single photons but also facilitate efficient photon extraction and manipulation.

Low-dimensional semiconductors such as self-assembled quantum dots (QD's) have great potential to serve as single-photon emitters due to their large oscillator strengths, two-level behavior, narrow spectral linewidths (<1 GHz), and their ease of integration with complex structures such as nanocavities.^{12,13} In this regard, the study of single QD's in high-index-contrast photonic crystals (PC's) has recently become an active area of research, which is largely due to the continued success in the fabrication of such structures.¹³ The ability to couple single QD's to nanophotonic materials and photonic dots is not only of fundamental importance but can also lead to novel applications including single-photon sources,¹⁴ low-threshold lasers,^{15–17} and optical amplifiers.¹⁸

To enhance the emission rate of a single-photon emitter, such as an atom or QD, it is well established that a modified electromagnetic vacuum of the surrounding environment can have a profound influence on the emission rates of a localized emitter. Thus, an increase in the local density of states (LDOS), created, for example, by a cavity, can lead to enhanced spontaneous emission through the Purcell effect.¹⁹ One drawback of using cavities to modify the LDOS is that the degree of control for cavity QED is typically limited to a

very narrow-band spectral region. However, since the pioneering works of Yablonovitch²⁰ and John,²¹ it is also known that periodic dielectric media such as PC's can create photonic band gaps that may substantially influence the LDOS that a photon feels over broadband frequencies. Lodahl *et al.*²² have reported LDOS enhancements in inverse opal structures. Baba *et al.*²³ have also demonstrated enhanced emission factors of greater than 16 at room temperature for PC point defects slab containing a GaInAsP quantum well. From a practical viewpoint, the planar semiconductor PC's currently show enormous promise since they exhibit large quality factors ($Q \sim 10^5$) and very small effective mode volumes ($V_{\text{eff}} \sim 0.05 \mu\text{m}^3$).^{24–27} Indeed, PC nanocavities are now facilitating new regimes of cavity QED.^{12,28–30}

To better exploit the single-photon emission potential of QD's in planar PC's, however, improvements in the microcavity excitation, enhanced cavity coupling, and efficient extraction of the emitted photons are all required. One possible vision that we propose here is that such a desired single-photon material structure (environment for emission) could be a waveguide rather than a cavity. While enhanced emission and “strong coupling” in *closed cavity* defect modes are to be expected, less obvious is what can be achieved with a propagating waveguide mode—an *open cavity*—where excitation and extraction can be extremely efficient and “all integration” is possible. Recently, signatures of spontaneous emission enhancement of single QD photon emission in a PC waveguide have been demonstrated experimentally,³¹ though the Purcell factors were rather modest since the QD was coupled to a leaky mode with a large effective mode volume. An increased LDOS for PC waveguides should not come as a great surprise since it has been predicted by Kleppner³² in 1981 that the emission of an emitter embedded in a wire waveguide may exhibit a divergentlike LDOS for frequencies lying near the waveguide cutoff and inhibition below the cutoff. This divergence physically comes from the one-dimensional (1D) propagation modes as the corresponding group velocity approaches zero, which can also be the case for planar PC waveguides.³³

The purpose of this paper is to explore in some detail the basic physics behind enhanced photon emission factors in planar PC waveguides, and then to carry out quantitative calculations and predictions for these structures. We have in mind applications that may use such structures for efficient

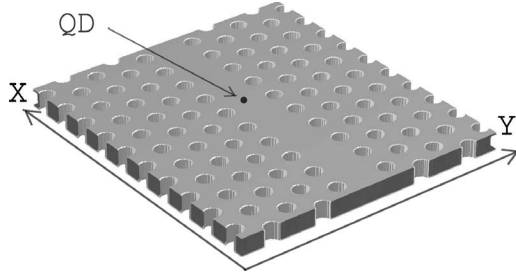


FIG. 1. Schematic showing a portion of the planar photonic crystal waveguide with a missing row of air holes creating a W1 waveguide along the x axis and an embedded single quantum dot (QD). The structure parameters to be used for calculations later are as follows: hole radius $r=0.275a$, slab thickness $0.5a$, refractive index $n=\sqrt{12}$, and lattice constant (pitch) $a=420$ nm.

photon generation and extraction. In contrast to what one might expect from nominal (non-PC) waveguides and open cavity systems, we show that pronounced Purcell factors can be achieved at certain spatial positions. Furthermore, large propagation mode β factors are obtained throughout the entire lossless propagation mode spectrum. These two quite remarkable features are strongly sought after properties in the continued development of efficient single-photon sources. We note that the β factor is usually defined in terms of conventional lasers, and so $\beta=1$ would correspond to all the spontaneous emission going into a lasing mode,³⁴ yielding the regime of “thresholdless lasing.” In this work, we define the single-photon β factor as the fraction of the emitted light that goes into a waveguide mode below the light line (with the rest being lost to radiation modes above the light line). Similar definitions have been used by Lecamp *et al.*³⁵ for describing dipole emission ratios in passive waveguides.

Our paper is organized as follows: In Sec. II, we introduce a photon Green-function formalism applicable for planar PC's and describe its use in determining the Purcell factor and waveguide mode β factor. In Sec. III, we present quantitative calculations for a W1 (removed array of holes) planar PC waveguide and study various dipole positions and orientations. In Sec. IV, we further discuss the consequences of our results and make a comparison with other nanostructures. Section V contains our conclusions.

II. THEORETICAL FORMALISM

Figure 1 depicts a schematic of a planar PC waveguide with a slab thickness approximately equal to $\sim\lambda/2n$, which is designed to support a broadband single waveguide mode below the light line. Our goal is to calculate the spontaneous emission rate from the embedded QD as a function of position and frequency into the various decay channels.

The general theory of spontaneous emission dates back more than a century to the pioneering work of Einstein. In 1905, Einstein first introduced the ideas of light-quanta,³⁶ and in 1917,³⁷ he applied statistical arguments to derive the rates of spontaneous and stimulated emissions, which are now known as the Einstein A and B coefficients, respec-

tively. For our present purpose, we are interested in exploring the underlying physics behind spontaneous emission, and thus we connect directly to the Einstein A coefficient. Throughout this work, we will deal exclusively with the “weak coupling regime,” as is appropriate for realistic waveguide structures, so we may naturally talk about Purcell factors. It should be noted, however, that an extension to general coupling (such as strong coupling) is straightforward within the formalism that we develop.

It is well known that spontaneous emission is induced by fluctuations in the electromagnetic-field vacuum. To account for the vacuum field, we first introduce the electric-field Green function tensor (GFT) $\mathbf{G}(\mathbf{r}, \mathbf{r}'; \omega)$, which describes the field response at \mathbf{r}' to an oscillating dipole at \mathbf{r} as a function of frequency. The GFT can be defined from Maxwell's equations, where

$$\left[\nabla \times \nabla \times - \frac{\omega^2}{c^2} \varepsilon(\mathbf{r}) \right] \mathbf{G}(\mathbf{r}, \mathbf{r}'; \omega) = \frac{\omega^2}{c^2} \mathbf{I} \delta(\mathbf{r} - \mathbf{r}'), \quad (1)$$

with \mathbf{I} the unit tensor (or dyadic) and $\varepsilon(\mathbf{r})$ the spatially dependent relative electric permittivity. The spontaneous emission rate (termed Γ , which is half the Einstein A coefficient) associated with population decay rate from an excited state $|1\rangle$ to the ground state $|0\rangle$ is³⁸

$$\Gamma(\mathbf{r}) = \frac{2\mathbf{d} \cdot \text{Im}[\mathbf{G}(\mathbf{r}, \mathbf{r}; \omega)] \cdot \mathbf{d}}{\hbar \varepsilon_0}, \quad (2)$$

where \mathbf{G} is the total GFT of the surrounding environment in which the two-state emitter (QD or atom) is embedded, and \mathbf{d} is the optical dipole of the QD. The decay from state $|1\rangle$ to state $|0\rangle$ results in the emission of a photon, whose properties depend not only on the emitter but also on the local environment through medium-dependent GFT.

With a proper separation of the quasitransverse and quasi-longitudinal electromagnetic modes, the GFT can be written as an expansion over the field modes in the system, so that

$$\mathbf{G}(\mathbf{r}, \mathbf{r}'; \omega) = \sum_{\mathbf{k}} \left[\frac{\omega^2}{\omega_{\mathbf{k}}^2 - \omega^2} \mathbf{E}_{\mathbf{k}}^T(\mathbf{r}) \mathbf{E}_{\mathbf{k}}^T(\mathbf{r}') + \mathbf{E}_{\mathbf{k}}^L(\mathbf{r}) \mathbf{E}_{\mathbf{k}}^L(\mathbf{r}') \right]. \quad (3)$$

We also define a modified GFT as

$$\mathbf{K}(\mathbf{r}, \mathbf{r}'; \omega) = \sum_{\mathbf{k}} \frac{\omega_{\mathbf{k}}^2}{\omega_{\mathbf{k}}^2 - \omega^2} \mathbf{E}_{\mathbf{k}}(\mathbf{r}) \mathbf{E}_{\mathbf{k}}(\mathbf{r}'), \quad (4)$$

where the modes from now on are all generalized transverse ($\mathbf{E}_{\mathbf{k}} = \mathbf{E}_{\mathbf{k}}^T$) and satisfy

$$\nabla \times \nabla \times \mathbf{E}_{\mathbf{k}}(\mathbf{r}) = \frac{\omega_{\mathbf{k}}^2}{c^2} \varepsilon(\mathbf{r}) \mathbf{E}_{\mathbf{k}}(\mathbf{r}). \quad (5)$$

By exploiting orthogonality, namely, $\delta(\mathbf{r} - \mathbf{r}') = \sum_{\mathbf{k}} \varepsilon(\mathbf{r}) \mathbf{E}_{\mathbf{k}}^{\alpha}(\mathbf{r}) \mathbf{E}_{\mathbf{k}}^{\alpha}(\mathbf{r}')$, where the sum includes all modes (physical and unphysical), the full GFT then becomes $\mathbf{G} = \mathbf{K} - \delta(\mathbf{r} - \mathbf{r}') / \varepsilon(\mathbf{r})$, and so $\Gamma \propto \text{Im}[\mathbf{K}]$. It is thus sufficient to work exclusively with \mathbf{K} , since its imaginary part is identical to the imaginary part of \mathbf{G} when $\mathbf{r} = \mathbf{r}'$. Similar GFT's have

been reported by Wubs *et al.*³⁹ using a multiple-scattering formalism.

For regular planar waveguide structures, as shown by Benisty *et al.*,⁴⁰ it is useful to separate out the various mode contributions in order to highlight the underlying mechanisms of spontaneous emission. We follow a somewhat similar strategy here for the purpose of making analytic progress with well established modes in the system. In general, the total GFT contains contributions from bound modes and radiation modes. One can write $\mathbf{K} = \mathbf{K}^{\text{bound}} + \mathbf{K}^{\text{rad}}$, and so the task is to obtain these mode contributions separately. Utilizing Bloch's theorem for periodic waveguides, the bound mode contribution to the GFT can be written as

$$\mathbf{K}^{\text{bound}}(\mathbf{r}, \mathbf{r}'; \omega) = \frac{ia\omega}{2v_g} [H(x-x')\mathbf{e}_{k_\omega}(\mathbf{r})\mathbf{e}_{k_\omega}^*(\mathbf{r}')e^{ik_\omega(x-x')} + H(x'-x)\mathbf{e}_{k_\omega}^*(\mathbf{r})\mathbf{e}_{k_\omega}(\mathbf{r}')e^{-ik_\omega(x-x')}], \quad (6)$$

where the first and second terms correspond to modes that are propagating forward and backward, respectively, H is the Heaviside function, $\mathbf{e}_{k_\omega}(\mathbf{r})$ is the propagating Bloch mode for wave vector k_ω , a is the pitch of PC waveguide, and $v_g = |v_g|$ is the corresponding group velocity. The fields are normalized through $\int_{\text{cell}} \varepsilon(\mathbf{r})|\mathbf{e}_{k_\omega}(\mathbf{r})|^2 d\mathbf{r} = 1$, carried over one unit cell of the periodic structure.

Once the GFT is known, the on-resonance Purcell factor can be obtained from

$$\text{PF}(r_d) = \frac{\mathbf{d} \cdot \text{Im}[\mathbf{K}^{\text{bound}}(r_d, r_d; \omega_d)] \cdot \mathbf{d}}{\mathbf{d} \cdot \text{Im}[\mathbf{G}^{\text{hom}}(\omega_d)] \cdot \mathbf{d}}, \quad (7)$$

where ω_d is the resonance energy of the QD, which can also include quantum corrections due to the vacuum field. Note that the Purcell factor PF is defined with respect to the bulk material GFT, where $\text{Im}[\mathbf{G}_{ii}^{\text{hom}}] = \omega^3 \sqrt{\varepsilon} / (6\pi c^3)$. From an embedded QD, the spontaneous emission rate in a bulk material then takes the familiar form $\Gamma = \omega_d^3 |\mathbf{d}|^2 \sqrt{\varepsilon} / (3\hbar \pi \varepsilon_0 c^3)$. The Purcell factor from the waveguide bound mode at the QD position ($\mathbf{r} = \mathbf{r}' = r_d$) can thus be derived analytically³³ as follows:

$$\text{PF}(r_d) = \frac{3\pi c^3 a |\mathbf{e}_{k_\omega}(r_d) \cdot \hat{\mathbf{n}}|^2}{\omega_d^2 \sqrt{\varepsilon} v_g}, \quad (8)$$

where $\hat{\mathbf{n}}$ is the unit vector along the orientation of the dipole and ε is the relative electric permittivity at the QD location. A first insight can be gained by noting that the Purcell factor contribution from the bound mode scales directly as the square of the field component in the dipole orientation at the QD's position. Secondly, the bound mode contribution scales inversely with the mode group velocity, so that large Purcell factors from an oscillating dipole are to be expected for slow-light modes.

To clarify further the physics behind the analytic waveguide PF [Eq. (8)], it is useful to introduce the concept of an effective mode volume, as is typically used when discussing cavity-QED. For a closed-system cavity with an effective mode volume V_{eff}^c and quality factor $Q = \omega_c / \Gamma_c$ (ω_c is the cavity resonance), one has

$$\text{PF}^c(r_d = r_{\text{antinode}}) = \frac{6\pi c^3 Q}{V_{\text{eff}}^c \omega_d^3 \varepsilon^{3/2}} = \frac{6\pi c^3}{V_{\text{eff}}^c \Gamma_c \omega_d^2 \varepsilon^{3/2}}, \quad (9)$$

for an on-resonance emitter ($\omega_d = \omega_c$) placed at the field antinode field position in the cavity. The effective mode volume for a PC waveguide, per unit cell, can also be defined as

$$V_{\text{eff}} = \frac{1}{\max(\varepsilon(\mathbf{r}))|\mathbf{e}_{k_\omega}(\mathbf{r})|^2}, \quad (10)$$

and so

$$\text{PF}(r_d = r_{\text{antinode}}) = \frac{3\pi c^3 a}{V_{\text{eff}} \omega_d^2 \varepsilon^{3/2} v_g} \quad (11)$$

or, in terms of an effective mode area,

$$\text{PF}(r_d = r_{\text{antinode}}) = \frac{3\pi c^3}{A_{\text{eff}} \omega_d^2 \varepsilon^{3/2} v_g}, \quad (12)$$

where $A_{\text{eff}} = V_{\text{eff}}/a$.

The connection between the cavity and waveguide enhanced emission now becomes clear. First, a reduced effective mode volume (per unit cell) can be realized if the pitch (a) is sufficiently small, and so this *effective* volume can be thought to be similar to the effective mode volume of a microcavity. The essential difference is that we are now dealing with a propagating mode in an infinite system, as opposed to a standing-wave mode confined in a closed system. Second, the decay rate of the cavity Γ_c is equivalent to the waveguide ratio $2v_g/a$, which tends toward zero at the PC band edge, or, equivalently, the quality factor of the waveguide $Q = a\omega/2v_g$. Surprisingly, the waveguide can have smaller effective mode volumes and smaller Γ_c (larger Q) than the confined cavities, but this is a theoretical consequence of having 1D-like periodic waveguide modes. Before elaborating on this point further, we conclude that the group velocity of the waveguide mode (when divided by the pitch) is somewhat equivalent to the cavity decay rate in a microcavity and that small effective mode volumes required for cavity QED can be realized in both open and closed systems (PC waveguides and cavities).

Does the LDOS for a three-dimensional (3D) structured waveguide really diverge? While a divergence from the real part of the GFT is well known and gives rise to established effects such as the Lamb shift,⁴¹ it may seem unphysical that the imaginary part of the GFT diverges (LDOS $\rightarrow \infty$), even for nonlossy dielectric media (ε is assumed to be real here). As remarked earlier in connection to the work of Kleppner,³² in the field of 1D-like (wire) waveguides, it has been predicted many years ago that the density of states (DOS) (and the LDOS) can diverge, even for an open system. Similar physics occurs here as the PC propagation mode is brought to a stop; we also note that radiation modes do not prevent this divergence as their contribution is physically well separated in k space. So, in a perfect infinitely long sample, there is a true divergence with the DOS and the LDOS in the planar PC waveguide. However, we add a few necessary works of caution. In reality, this divergence will never occur due to various effects, such as a finite length sample, struc-

tural disorder, and radiative decay of any embedded photon emitter. For certain spatial locations, the field mode may also be zero. Most importantly, the effects of slow group velocity on disorder-induced scattering loss have been shown to have a profound impact on planar PC waveguides,^{42–45} as well as on PC's in general.⁴⁶ In this context, the open systems do suffer more strongly from the influence of sample disorder and surface roughness. To make this point clearer, the LDOS resonance broadens more strongly in an open system due to sample imperfections. In either system, we note that one can include realistic imperfections by using a Born-approximation for the GFT,^{42,43} which is valid for weak disorder.

We also define the single-QD (or single-photon) β factor which gives a measure of the probability of a photon being emitted into a (desired) waveguide mode; the waveguide mode of interest is “lossless” (at least in theory) and so will be contained within the planar structure. The propagation mode β factor can be written as

$$\beta = \frac{\Gamma_{\text{bound}}}{\Gamma_{\text{bound}} + \Gamma_{\text{rad}} + \Gamma_{\text{nr}}}, \quad (13)$$

which applies to a photon emitter within a cavity or a waveguide. The Γ_{rad} is related to the spontaneous emission into a continuum of radiation and/or leaky modes, and Γ_{nr} is the nonradiative decay rate due to various dephasing processes associated with the emitter (atom or QD). A β factor of 1 thus corresponds to a 100% probability of emitting a photon into the waveguide mode. Since the emphasis in this work is on radiative decay rates, we will neglect the nonradiative decay since for typical QD's its contribution is known to be small at low temperatures, with $\Gamma_{\text{nr}} \sim$ sub gigahertz.⁴⁷ In comparing to actual experiments, however, one should include this term if fitting to measurements as a function of temperature.

III. CALCULATIONS

Since we have in mind applications toward single-photon emission and extraction, we focus our analysis to the spontaneous emission arising from a single embedded QD within a planar PC waveguide. For the purpose of manipulating the LDOS for light extraction, a closed cavity system usually only facilitates collection over a very narrow band of frequencies (as expected for a cavity-QED regime). On the contrary, we will show that the PC waveguides offer some unique broadband behavior. At first sight, the investigation of photon emission from an infinite 3D planar waveguide with a periodic lattice of air holes seems like a formidable problem; since even for regular ridge waveguide, the calculation of emission rates is a highly nontrivial and difficult task.^{31,40} However, for PC waveguides the Bloch mode theory helps simplify the analysis considerably. Indeed, as we will show below, since the bound mode contribution dominates the GFT, the analytic PC theory presented above is an excellent approximation for the Purcell factor over the entire spectrum of the lossless propagation mode.

We consider a typical triangular lattice of air holes on an air-bridged semiconductor slab, where a standard W1 waveguide (cf. Fig. 1 earlier) is formed by removing one row of

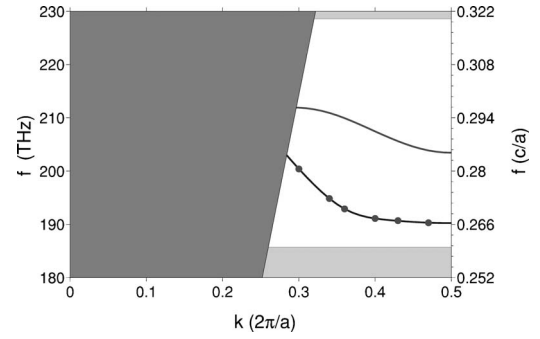


FIG. 2. Photonic crystal waveguide band structure within the TE-like band gap, showing the bound modes below the light line (solid curves) and the continuum of radiation modes (dark shaded regions above the light line).

air holes in the propagation direction. In Fig. 2, we show the corresponding band structure of the fundamental and higher-order modes of the W1 waveguide lying within the TE-like band gap (spanning about 185–228 THz or 0.26–0.32 c/a in scaled frequency units); also shown is the continuum of radiation modes above the light line. For large k values, at the band edge of the fundamental mode, the group velocity becomes small which corresponds to slow-light propagation. The shaded region above the light line represents a continuum of radiation modes and leaky modes if they exist; all of these modes contribute to the $\mathbf{K}^{\text{rad}}(\mathbf{r}, \mathbf{r}', \omega)$, which does not lend itself to a simple analytic expression. Importantly, below the light line, there is clearly a large frequency range (about 10 THz or 80 nm) in which the waveguide is single mode.

Experimentally, the QD's can be made to interact optimally with the waveguide mode by spatial and spectral tuning.¹² To understand the basic mechanisms of photon emission in PC waveguides, we first study the different components of the mode profiles for specific Bloch wave vectors. This allows us to gain insight into the expected scaling behavior of the Purcell factors with respect to the emitter's position and frequency. In Fig. 3(a), we show an example of the field distribution of guided mode E_y —component of the guided mode with relatively slow group velocity [at $k_\omega = 0.47 (2\pi/a)$ with $v_g \sim c/154$] for one unit cell of the waveguide where most of the energy is localized (within the center of the slab). We choose this wave vector as a typical upper k limit (smaller group velocity) that can be measured experimentally.^{25,48} The corresponding effective mode volume is only $V_{\text{eff}} = 0.03 \mu\text{m}^3$, which is notably *smaller* than most PC nanocavity mode volumes reported to date. The effective mode volumes of the broadband waveguide modes are in the range 0.02–0.03 μm^3 , which correspond to waveguide k values of 0.3–0.48 ($2\pi/a$).

We also present an example “spatial map” of the Purcell factor for a y -polarized dipole [see Fig. 3(b)] as a function of QD position on a plane parallel to the slab for $k_\omega = 0.47 (2\pi/a)$. As can be recognized, substantial enhancements in the spontaneous emissions rate by up to a factor of 30 are achievable, which become even greater for smaller group velocities. Although the group-velocity enhancements have been discussed before by Hughes for the antinode position

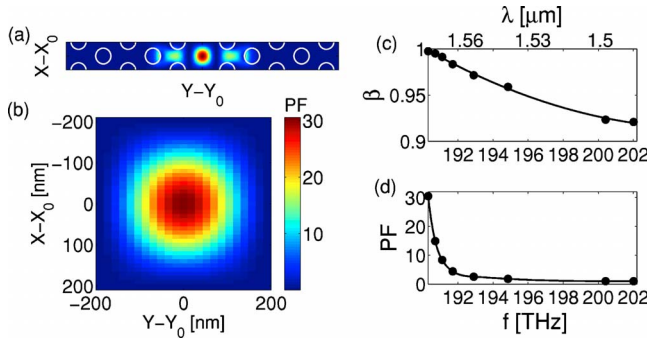


FIG. 3. (Color online) (a) Example of electric-field profile of y component ($|e^y(\mathbf{r})|^2$) of a slow-light mode on the plane parallel to the slab and located at midplane of the slab ($z=0$) shown for one unit cell; the wave vector is $k=0.47(2\pi/a)$ and the corresponding group index $n_g=154$. The superimposed white circles show boundaries of air holes in the slab. (b) Purcell factor (PF) as a function of QD position on the same plane as in (a) for a slow-light mode with dipole orientation along the y axis. (c) β factor as a function of fundamental mode frequency for the case of y -oriented dipole positioned at the field antinode. (d) The corresponding Purcell factor.

only³³ (see also Viasnoff-Schwob *et al.*³¹), in this work, we want to emphasize the important influence of spatial positioning and to analyze in detail the influence of the dipole direction and the contribution from the radiation modes. As can be seen, if the same dipole was placed away from the antinode position, the Purcell factor would reduce substantially as it scales with the field strength squared. Thus, there is a “hot spot” area of around $\pi(80 \text{ nm})^2=0.02 \mu\text{m}^2$ that yields Purcell factors of greater than 20.

In order to determine the amount of spontaneous emission that is lost to radiation modes above the light line, we have performed detailed finite-difference time-domain (FDTD) simulations⁴⁹ for this structure to make a rigorous calculation of the radiation mode continuum contribution to \mathbf{G} , namely \mathbf{G}^{rad} . To do this, we excite a dipole at the desired spatial point and compute the total GFT and the radiation mode contribution to the GFT directly, which can be obtained from a finite-size sample. Similar techniques have been used to successfully describe extrinsic scattering loss in PC waveguides.^{42,43} For example, at the antinode spatial position shown in the calculated PF map, the LDOS contribution $\text{Im}[\mathbf{G}_{yy/xx}^{\text{rad}}] \approx 0.06-0.09 \text{ Im}[\mathbf{G}_{jj}^{\text{hom}}]$ in the frequency range of interest. This confirms the large effect of the PC band gap, namely, since we are deep in the photonic band gap, the coupling to radiation modes is substantially reduced in comparison with a homogeneous structure. The bound mode β factor, which we have defined earlier, can then be calculated as a function of frequency and the results are shown in Fig. 3(c). The bound mode contribution is obtained analytically (but using computed modes and group velocities), while the radiation mode contribution is computed numerically. The filled circles in the figure show the calculations performed for specific frequencies and then interpolated with a best-fit curve to depict the whole frequency range associated with the fundamental propagation mode below the light line [see the band diagram of Fig. 2]. The corresponding Purcell factor dependence on the mode frequency at this spatial position

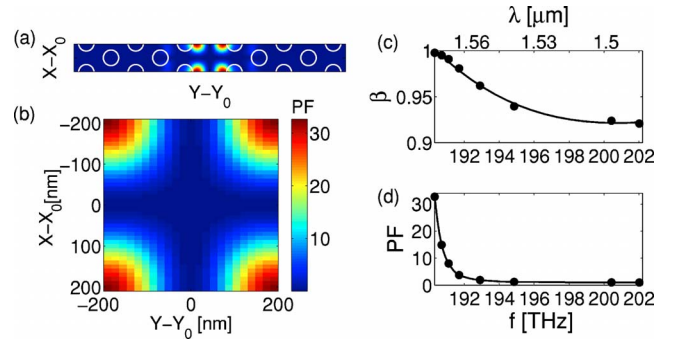


FIG. 4. (Color online) (a) Example of electric-field profile of the x component ($|e^x(\mathbf{r})|^2$) using identical parameters as in Fig. 3. (b) Purcell factor (PF) as a function of QD position on the same plane as in (a) for a slow-light mode with the dipole orientation along the x axis. (c) β factor as a function of fundamental mode frequency for the case of x -oriented dipole positioned at one of the field antinodes. (d) The corresponding Purcell factor.

is shown in Fig. 3(d), which, as expected, tends toward 1 for the smaller k (larger ω).

Next, we carry out an investigation using the E_x —component of the guided mode. The corresponding field profile is shown in Fig. 4(a), which now has four symmetric antinodes in stark contrast to the one antinode obtained for the y component within the same unit cell. Again, we have a very low effective mode volume of $V_{\text{eff}}=0.029 \mu\text{m}^3$. The x -oriented dipole placed at one of these antinodes gives a maximum Purcell factor of 33 using the same slow-light mode with a corresponding wave vector $k=0.47(2\pi/a)$. In Fig. 4(b) we show the spatial dependence of the rate enhancements in the center plane of the slab, and it is noted that the Purcell factor is maximum if the dipole is placed close to the air holes. The corresponding β factors and Purcell factors as a function of mode frequency are shown in Figs. 4(c) and 4(d), respectively, with the QD positioned at one of these four antinodes.

In practice, the dipole orientation (polarization) of a QD embedded in a planar PC waveguide can be random (but still predominantly polarized in the plane for self-assembled semiconductor QD's). For completeness, we show in Fig. 5(a) the spatial map for the case when the orientation is at 45° with respect to the x and y axes. The Purcell factor effectively reduces by a factor of 2 in comparison with ideal cases shown in Figs. 3(b) and 4(b). Figures 5(b) and 5(c) display the corresponding β factor and Purcell factor, respectively, as a function of frequency for a dipole at two different antinodes, namely, at the center (circles) and at the edge (crosses) of the waveguide.

IV. DISCUSSION

We have introduced a PC waveguide formalism that predicts large spectrally-sharp Purcell factors and impressive broadband β factors. While being polarization dependent, typically one can expect greater than 85% coupling efficiency channeled into the waveguide mode over a large spectral range of 10 THz (about 80 nm in wavelength). Certain

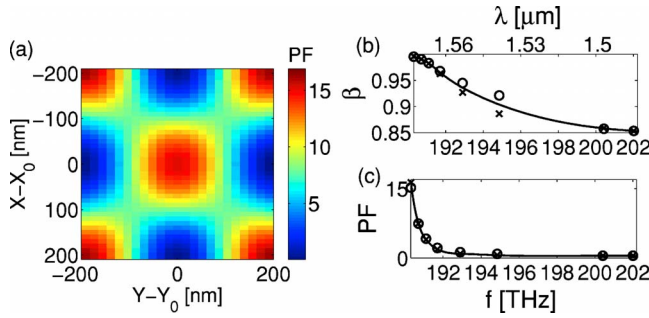


FIG. 5. (Color online) (a) Spatial map of the Purcell factor as function of QD position on the same plane as in Fig. 3(b) (center of the slab) for the case when the dipole orientation is 45° with respect to the x or y axes. The other parameters remain the same as those used in Fig. 3(b) or 4(b). (b) β factors as a function of fundamental mode frequency for two different dot positions (center antinode and corner antinode shown by the crosses and circles, respectively). (c) The corresponding Purcell factors.

spatial positions are dominated by E_x , others by E_y , and some by $E_x \approx E_y$; the latter scenario is a case that we have not highlighted, but it may have some uses, e.g., in producing correlated photon pairs from biexciton and/or exciton states in semiconductor QD's. Taking all these properties together, we are not aware of any other structure that can achieve such bound mode functionality. For amplifying and lasing applications, where the β factor was probably first invented, lasing in PC waveguides would likely be unstable due to the sensitive frequency dependence of the Purcell factor. However, there may be some clever designs that could enable broadband Purcell factors in waveguides given the suitable motivation that has been highlighted here.

With regard to single-photon emission and extraction, we believe that the results seem quite promising from both fundamental physics and applied perspectives. Though we have specialized the analysis for frequencies that closely correspond to telecom wavelengths, we highlight that the results and conclusions remain qualitatively the same for other wavelengths typical of single semiconductor QD's. For example, for a wavelength of $\lambda \sim 1.27 \mu\text{m}$ (≈ 240 THz), and again using the slow-light mode with corresponding wave vector $k=0.47$ ($2\pi/a$), the calculated Purcell factors are 28 and 31 for y -oriented and x -oriented dipoles, respectively. Once more, the coupling of emitted photons to radiation modes is suppressed, leading to β factors greater than 0.99 for this wavelength and similar broadband enhancements over the lossless propagation mode spectral region. In the slow-light regime, the group-velocity dispersion and extrinsic scattering loss may also become problematic for sufficiently long waveguides.

We also clarify a subtle and interesting point regarding the chosen direction of the emitted photon, if it is emitted into a waveguide mode. The Purcell factor as defined in this paper sums over the backward and forward waveguide propagation modes. Statistically, the photon if emitted into the desired waveguide mode will go one way or the other 50% of the time, but with one event at a time. If one desires to send the

photon a particular way close to 100% of the time (we neglect the influence of radiation modes for the purpose of this discussion), a reflector can be added within the path of the filtered out direction at the appropriate position. The “appropriate position” would naturally exploit the Bloch mode phase in such a way as to maximize reflection, namely, when $e^{\pm i2k_\omega(x_d - x_m)} = 1$, where x_d is the x position of the dipole and x_m is the x position of the downstream (or upstream) reflector. More elaborate schemes could feasibly couple in frequency-dependent reflectors (side-coupled cavities, for instance) to control which way the photon would go. Regardless of the details of the well separated reflector, it can be conveniently added into the total GFT through the Dyson equation.^{28,50}

We briefly make some comparisons with single QD experiments that try to maximize single-photon emission and extraction with cavities.^{51–53} Chang *et al.*⁵³ have reported a Purcell factor of 3 and a β factor of 0.92 for an InGaAs QD in a PC nanocavity with a $Q \sim 300$. However, the collection efficiency is only 10%–20%. Pelton *et al.*⁵² have reported a Purcell factor of 5.8 and a β factor of 0.83 using a micropost cavity of $0.6 \mu\text{m}$ in diameter and $4.2 \mu\text{m}$ in height with a $Q \sim 627$; here the collection efficiency is 38%. While the β factors in both these experiments are 2 orders greater than that of a single QD in bulk semiconductor, the photon collection efficiency and bandwidth considerations (the bound modes are spectrally sharp) have undermined these impressive enhancements and efficiency factors. In contrast, our scheme offers reasonably large Purcell factors (also narrow band) and facilitates large β factors and collection efficiencies over a massive 80 nm (10 THz) bandwidth. Moreover, recent reports suggest that it is possible to insert and extract light from PC waveguides via evanescent coupling of a tapered fiber with an efficiency of up to 98%.⁵⁴

V. CONCLUSIONS

In summary, a rigorous and physically intuitive theoretical formalism to investigate single quantum-dot Purcell factors and propagation mode β factors in planar PC waveguides has been introduced. We have highlighted the influence of dipole orientation and position within the unit cell of the waveguide and made a connection to Purcell factors in microcavities. In terms of single-photon applications, we predict impressive Purcell factors for realistic slow light modes and enhanced propagation mode β factors (>0.85) over a wide spectral range (10 THz or ~ 80 nm). These results may have important applications toward the development of efficient single photon sources for quantum information science and are of fundamental interest in the domains of quantum optics and nanophotonics.

ACKNOWLEDGMENTS

We thank H. Benisty, L. Ramunno, T. Baba, and A. Legendijk for useful discussions. This work was supported by the Natural Sciences and Engineering Research Council of Canada, the Canadian Foundation for Innovation, and the Ministry of Research and Innovation, Ontario.

*Electronic address: shughes@physics.queensu.ca

- ¹W. Yao, R.-B. Liu, and L. J. Sham, Phys. Rev. Lett. **95**, 030504 (2005).
- ²D. Fattal, E. Diamanti, K. Inoue, and Y. Yamamoto, Phys. Rev. Lett. **92**, 037904 (2004).
- ³E. Knill, R. Laflamme, and G. Milburn, Nature (London) **409**, 46 (2001).
- ⁴N. Yoran and B. Reznik, Phys. Rev. Lett. **91**, 037903 (2003).
- ⁵A. Beveratos, R. Brouri, T. Gacoin, A. Villing, J.-P. Poizat, and P. Grangier, Phys. Rev. Lett. **89**, 187901 (2002).
- ⁶B. Lounis and M. Orrit, Rep. Prog. Phys. **68**, 1129 (2005).
- ⁷J. McKeever, A. Boca, A. D. Boozer, R. Miller, J. R. Buck, A. Kuzmich, and H. J. Kimble, Science **303**, 1992 (2004).
- ⁸C. Brunel, B. Lounis, P. Tamarat, and M. Orrit, Phys. Rev. Lett. **83**, 2722 (1999).
- ⁹B. Lounis and W. E. Moerner, Nature (London) **407**, 491 (2000).
- ¹⁰C. W. Chou, S. V. Polyakov, A. Kuzmich, and H. J. Kimble, Phys. Rev. Lett. **92**, 213601 (2004).
- ¹¹M. Keller, B. Lange, K. Hayasaka, W. Lange, and H. Walther, Nature (London) **431**, 1075 (2004).
- ¹²A. Badolato, K. Hennessy, M. Atature, J. Dreiser, E. Hu, P. M. Petroff, and A. Imamoglu, Science **308**, 1158 (2005).
- ¹³P. Michler, Top. Appl. Phys. **90**, 352 (2003).
- ¹⁴C. Santori, M. Pelton, G. Solomon, Y. Dale and Y. Yamamoto, Phys. Rev. Lett. **86**, 1502 (2001).
- ¹⁵M. Loncar, T. Yoshie, A. Scherer, P. Gogna, and Y. Qiu, Appl. Phys. Lett. **81**, 2680 (2002).
- ¹⁶S. Reitzenstein, A. Bazhenov, A. Gorbunov, C. Hofmann, S. Münch, A. Löffler, M. Kamp, J. P. Reithmaier, V. D. Kulakovskii, and A. Forchel, Appl. Phys. Lett. **89**, 051107 (2006).
- ¹⁷S. Anantathanasarn, R. Nötzel, P. J. van Veldhoven, F. W. M. van Otten, Y. Barbarin, G. Servanton, T. de Vries, E. Smalbrugge, E. J. Geluk, T. J. Eijkemans, E. A. J. M. Bente, Y. S. Oei, M. K. Smit, and J. H. Wolter, Appl. Phys. Lett. **89**, 073115 (2006).
- ¹⁸A. J. Zilike, J. Meier, P. W. E. Smith, M. Mojahedi, J. S. Aitchison, P. J. Poole, C. N. Allen, P. Barrios, and D. Poitras, Opt. Express **14**, 11453 (2006).
- ¹⁹E. M. Purcell, Phys. Rev. **69**, 681 (1946).
- ²⁰E. Yablonovitch, Phys. Rev. Lett. **58**, 2059 (1987).
- ²¹S. John, Phys. Rev. Lett. **58**, 2486 (1987).
- ²²P. Lodahl, A. F. Van Driel, I. N. Nikolaev, A. Irman, K. Overgaag, D. Vanmaekelbergh, and W. L. Vos, Nature (London) **430**, 654 (2004).
- ²³T. Baba, D. Sano, K. Nozaki, K. Inoshita, Y. Kuroki, and F. Koyama, Appl. Phys. Lett. **85**, 3989 (2004).
- ²⁴Y. Akahane, T. Asano, B. S. Song, and S. Noda, Nature (London) **425**, 944 (2003).
- ²⁵E. Kuramochi, M. Notomi, S. Mitsugi, A. Shinya, T. Tanabe, and T. Watanabe, Appl. Phys. Lett. **88**, 041112 (2006).
- ²⁶E. Weidner, S. Combria, N.-V.-Q. Tran, A. De Rossi, J. Nagle, S. Cassette, A. Talneau, and H. Benisty, Appl. Phys. Lett. **89**, 221104 (2006).
- ²⁷S. Frederick, D. Dalacu, J. Lapointe, P. J. Poole, G. C. Aers, and R. L. Williams, Appl. Phys. Lett. **89**, 091115 (2006).
- ²⁸S. Hughes, Phys. Rev. Lett. **98**, 083603 (2007).
- ²⁹K. Hennessy, A. Badolato, M. Winger, A. Atature, S. Falt, E. L. Hu, and A. Imamoglu, Nature (London) **445**, 896 (2007).
- ³⁰T. Yoshie, A. Scherer, J. Hendrickson, G. Khitrova, H. M. Gibbs, G. Rupper, C. Ell, O. B. Shchekin, and D. G. Deppe, Nature (London) **432**, 200 (2004).
- ³¹E. Viasnoff-Schwoob, C. Weisbuch, H. Benisty, S. Olivier, S. Varoutsis, I. Robert-Philip, R. Houdre, and C. J. M. Smith, Phys. Rev. Lett. **95**, 183901 (2005).
- ³²D. Kleppner, Phys. Rev. Lett. **47**, 233 (1981).
- ³³S. Hughes, Opt. Lett. **15**, 2659 (2004).
- ³⁴Y. Yamamoto, S. Machida, and G. Bjork, Phys. Rev. A **44**, 657 (1991).
- ³⁵G. Lecamp, P. Lalanne, and J. P. Hugonin, Proc. SPIE **6195**, 61950E (2006).
- ³⁶A. Einstein, Ann. Phys. **17**, 132 (1905).
- ³⁷A. Einstein, Phys. Z. **18**, 121 (1917).
- ³⁸See, e.g., H. T. Dung, L. Knöll, and D.-G. Welsch, Phys. Rev. A **62**, 053804 (2000).
- ³⁹M. Wubs, L. G. Suttorp, and A. Lagendijk, Phys. Rev. A **70**, 053823 (2004).
- ⁴⁰H. Benisty, R. Stanley, and M. Mayer, J. Opt. Soc. Am. A **15**, 1192 (1998).
- ⁴¹See, e.g., H. A. Bethe, Phys. Rev. **72**, 339 (1947); for a textbook discussion, see M. O. Scully and M. S. Zubairy, in *Quantum Optics* (Cambridge University Press (1997)).
- ⁴²S. Hughes, L. Ramunno, Jeff F. Young, and J. E. Sipe, Phys. Rev. Lett. **94**, 033903 (2005).
- ⁴³E. Kuramochi, M. Notomi, S. Hughes, A. Shinya, T. Watanabe, and L. Ramunno, Phys. Rev. B **72**, 161318(R) (2005).
- ⁴⁴M. L. Povinelli, S. G. Johnson, E. Lidorikis, J. D. Joannopoulos, and M. Soljacic, Appl. Phys. Lett. **84**, 3639 (2004).
- ⁴⁵D. Gerace and L. C. Andreani, Opt. Lett. **29**, 1897 (2004).
- ⁴⁶A. F. Koenderink, Ad Lagendijk, and W. L. Vos, Phys. Rev. B **72**, 153102 (2005).
- ⁴⁷W. Langbein, P. Borri, U. Woggon, V. Stavarache, D. Reuter, and A. D. Wieck, Phys. Rev. B **70**, 033301 (2004).
- ⁴⁸Y. A. Vlasov, M. O. Boyle, H. F. Hamann, and S. J. McNab, Nature (London) **438**, 65 (2005).
- ⁴⁹We have used FDTD Solutions, by Lumerical Solutions Inc., www.lumerical.com.
- ⁵⁰A. R. Cowan and Jeff F. Young, Phys. Rev. E **68**, 046606 (2003).
- ⁵¹A. Kress, F. Hofbauer, N. Reinelt, M. Kaniber, H. J. Krenner, R. Meyer, G. Bohm, and J. J. Finley, Phys. Rev. B **71**, 241304(R) (2005).
- ⁵²M. Pelton, C. Santori, J. Vuckovic, B. Zhang, G. S. Solomon, J. Plant, and Y. Yamamoto, Phys. Rev. Lett. **89**, 233602 (2002).
- ⁵³W.-H. Chang, W.-Y. Chen, H.-S. Chang, T.-P. Hsieh, J.-I. Chyi, and T.-M. Hsu, Phys. Rev. Lett. **96**, 117401 (2006).
- ⁵⁴C. Grillet, C. Smith, D. Freeman, S. Madden, B. L.-Davies, E. C. Magi, D. J. Moss, and B. J. Eggleton, Opt. Express **14**, 1070 (2006).